Inorganic Chemistry

ARTICLE

pubs.acs.org/IC

Metal Binding Ability of Cysteine-Rich Peptide Domain of ZIP13 Zn^{2+} Ions Transporter

Slawomir Potocki,[†] Magdalena Rowinska-Zyrek,[†] Daniela Valensin,[‡] Karolina Krzywoszynska,[†] Danuta Witkowska,[†] Marek Luczkowski,[†] and Henryk Kozlowski*[,†]

[†]Faculty of Chemistry, University of Wroclaw, F. Joliot-Curie 14, 50-383 Wroclaw, Poland

[‡]Department of Chemistry, University of Siena, Via Aldo Moro 2, Siena 53100, Italy

ABSTRACT: The coordination modes and thermodynamic stabilities of the complexes of the cysteine-rich N-terminal domain fragment of the ZIP13 zinc transporter (MPGCPCPGCG−NH_2) with Zn^{2+}, Cd^{2+}, Bi^{3+}, and Ni^{2+} have been studied by potentiometric, mass spectrometric, NMR, CD, and UV−vis spectroscopic methods. All of the studied metals had similar binding modes, with the three thiol sulfurs of cysteine residues involved in metal ion coordination. The stability of the complexes formed in solution changes in the series $Bi^{3+} \gg Cd^{2+} > Zn^{2+} > Ni^{2+}$, the strongest being for bismuth and the weakest for nickel. The N-terminal fragment of the human metalothionein-3 (MDPETCPCP−NH_2) and unique histidine- and cysteine-rich domain of the C-terminus of *Helicobacter pyroli* HspA protein (Ac−ACCHDHKKH−NH_2) have been chosen for the comparison studies. It confirmed indirectly which groups were the anchoring ones of ZIP13 domain. Experimental data from all of the used techniques and comparisons allowed us to propose possible coordination modes for all of the studied ZIP13 complexes.

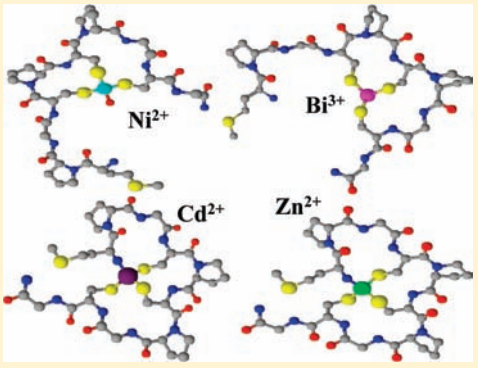

INTRODUCTION

There is strong evidence that transmembrane ZIP proteins (SLC39) are evolutionarily related and possess functional and structural similarities to prion proteins,[1] which are able to undergo transformation into the pathogenic insoluble scrapie form, responsible for neurodegenerative disorders and thus neurodegenerative diseases.[2,3] Previous studies on ZIP proteins are related to cell biology and the application of ^{65}Zn radioisotope[4,15] or emission fluorescence for zinc trafficking studies.[5] As far as we may realize, the knowledge on thermodynamics and coordination chemistry of metal complexes of SLC39 proteins is elusive. A possible function of PrPs may be obtained through the characterization of its molecular neighborhood in cells.[1] The characterization of the function, types of interactions, coordination modes, thermodynamic stabilities of complexes of various metal ions with ZIP proteins, and their molecular structures will allow a deeper understanding of the mechanisms of action associated with prion proteins during both illness and health.

ZIP proteins are responsible for the increase of zinc concentration within the cell cytoplasm, whether derived from extracellular fluid or from intracellular vesicles.[6−8] Among the ZIP family of proteins, we distinguish 14 members deployed in different parts of the cell.[9−11] The transport of zinc by hZIP1 and hZIP2, members of the human SLC39 family, does not require ATP and is induced by HCO_3^-.[12,13] Metal competition studies indicate some mammalian SLC39 proteins are specific for zinc;[14] however, for some ZIP proteins, zinc uptake activity was found to be inhibited by many cations.[15] Despite many attempts to explain the mechanism of metal ion transport across the biological membrane carried out by ZIP proteins, it still remains a controversial issue.

Proteins that contain histidine- and/or cysteine-rich domains in their primary structure efficiently bind zinc and other divalent metal cations;[16] for example, Zn^{2+} ions bind very efficiently to the histidine-rich tandem repeat region of "prion related protein" (PrP-rel-2) of zebra-fish,[17] whereas the C-terminus of HspA protein (crucial for nickel homeostasis in *Helicobacter pylori* bacteria) efficiently binds both native nickel and inhibitory bismuth.[18] Studies on the interactions of such cysteine-rich sequences with metal ions are critical for understanding the possible biological function of the proteins which they are part of.

The main objective of our studies is the evaluation of metal ion binding properties of the N-terminal domain fragment of the ZIP13 zinc transporter versus Zn^{2+}, Bi^{3+}, and Ni^{2+}. ZIP proteins play an important role in the uptake of cadmium in mammalian cells;[19] moreover, cadmium ions can bind to zinc binding sites in ZIP transporters and cause damage to testis and kidney,[20] therefore the binding mode of Cd^{2+} was studied as well. The interactions of Ni^{2+} and Bi^{3+} with Cys-rich proteins are also of particular interest, because of the enormous amount of such in *H. pylori*. Cys-rich proteins are essential for the bacteria, because they are responsible for the homeostasis of Ni^{2+}, crucial for the dinuclear Ni^{2+}-containing enzyme urease, which catalyzes the hydrolysis of urea into carbon dioxide and ammonia and

Received: February 8, 2011
Published: June 01, 2011

therefore neutralizes the low gastric pH around the bacteria, and a membrane-bound [NiFe] hydrogenase, which permits respiratory-based energy production for the bacteria in the mucosa.[21] Bismuth-based drugs are successful therapeutic agents against *H. pylori* infections. Most probably, Bi^{3+} is an inhibitor of those Cys-rich nickel homeostasis proteins, although its exact mechanism of action is not completely clear. It is postulated that it might displace Ni^{2+} from its binding site, and, because of this, the interactions of both metals with cysteine-rich peptides are intensively studied.

The studied decapeptide is the N-terminal sequence of the human ZIP13 zinc transporter protein (of its naturally occurring isoform 1 and 2, 371, and 364 aminoacid residues, respectively). This protein is located mainly in Golgi apparatus, but also in the perinuclear region of osteoblasts, chondrocytes, pulpal cells, and fibroblasts, suggesting that Slc39a13 protein may function as an intracellular Zn^{2+} transporter in connective tissue forming cells.[22] It possess eight transmembrane domains and extracellular/cytoplasmic loops between them. Some of the loops are expected to be responsible for selectivity of the protein toward different metal ions, although there is still lack of reliable information concerning this issue. The N-terminal sequence is interesting mainly from the chemical point of view as a multicysteine peptide ligand. Such ligands can be coordinated differently depending on the vicinal aminoacid environment; therefore, multicysteine sequences that occur naturally are those of great interest.

EXPERIMENTAL SECTION

Peptide Synthesis, Purification, and Characterization. Peptides were synthesized with an Activotec Activo-P11 automated peptide synthesizer, with Fmoc-protected amino acids using Fmoc chemistry. Rink-amide resin was used as the solid support so that the resulting peptides would be amidated at the C-terminus. The N-terminus was acetylated with a solution of 1 M acetic anhydride, 0.4 M diisopropylethylamine in *N*,*N*-dimethylformamide (DMF). Cleavage from the resin was performed for 90 min in a 90% trifluoroacetic acid (TFA) solution containing 5% thioanisole, 2% anisole, and 3% ethanedithiol as free radical scavengers. After precipitation with cold ether, the peptides were redissolved in water and lyophilized to obtain a fluffy off-white powder. The solid was redissolved in 10% acetic acid and purified by reversed phase HPLC on a Varian Prostar HPLC with a preparative C18 column (Varian Pursuit XRs C 18) with a semilinear gradient of 0.1% TFA in water to 0.1% TFA in acetonitrile 9:1 CH_3CN/H_2O over 45 min. The purity of peptides was verified by ESI (electrospray ionization) mass spectrometry.

UV−Vis and CD Measurements. The absorption spectra were recorded on a Cary 300 Bio spectrophotometer, and circular dichroism (CD) spectra were recorded on Jasco J715 spectropolarimeter in the 800−230 nm range. For the Ni^{2+} complex, the ligand concentration was 1×10^{-3} M, and the metal to ligand molar ratios were 1:2 and 1:1.1; as for Cd^{2+}, the ligand concentration was 1.1×10^{-4} M, and the Cd^{2+} to ligand molar ratio was 1:1.1 for UV−vis, the ligand concentration was 1 mM, and the metal to ligand molar ratios were 1:2 and 1:1.1 for CD spectroscopy; as for the Bi^{3+} species, the ligand concentration was 1.25×10^{-4} M, and the Bi^{3+} to ligand molar ratio was 1:2. The formation equilibria of Bi^{3+}−ligand complexes, which occur in the 0.2−2.5 pH range, were studied on a set of batch titrations in a step of 0.1, at 298 K using a total volume of 2 mL. The complex formation constants and the absorptivity spectra were calculated with the Specfit program,[23,24] which fits the stability constants and the corresponding molar extinction coefficients (M^{-1} cm^{-1}) of the species.

Table 1. ^1H and ^{13}C Chemical Shift Assignments of MPGCPCPGCG−NH_2, 0.003 M, pH 5.0, *T* 298 K

residue	^1H	δ chemical shift (ppm)	^{13}C	δ chemical shift (ppm)
Met-1	Hα	4.5	Cα	54.1
	Hβ	2.21	Cβ	32.4
	Hγ	2.68	Cγ	31.2
	Hε	2.11	Cε	17.3
Pro-2	Hα	4.5	Cα	63.8
	Hβ	2.34; 1.97	Cβ	32.4
	Hγ	2.08	Cγ	27.7
	Hδ	3.79; 3.67	Cδ	51.5
Gly-3	NH	8.58		
	Hα	3.97	Cα	45.4
Cys-4	NH	8.11		
	Hα	4.85	Cα	56.9
	Hβ	2.9	Cβ	28.0
Pro-5 = Pro-7	Hα	4.44	Cα	63.8
	Hβ	2.31; 2.00	Cβ	32.4
	Hγ	2.08	Cγ	27.7
	Hδ	3.78	Cδ	51.1
Cys-6	NH	8.44		
	Hα	4.81	Cα	56.9
	Hβ	2.93	Cβ	28.0
Gly-8	NH	8.52		
	Hα	4.01	Cα	45.4
Cys-9	NH	8.24		
	Hα	4.57	Cα	59.0
	Hβ	2.99	Cβ	28.5
Gly-10	NH	8.55		
	Hα	3.95	Cα	45.4

All spectroscopic measurements were performed under argon, and all solutions used in this study were deaerated, because of the possible oxidation of the cysteine groups.

Potentiometric Measurements. All data were calculated from three titrations carried out over the pH range 2.5−10.5 at 298 K in 0.1 M KCl using a total volume of 2 mL on a MOLSPIN pH-meter system using a Russel CMAW 711 semicombined electrode calibrated in proton concentrations using HCl.[25] All potentiometric measurements were performed under argon, and all solutions used in this study were deaerated, because of the possible oxidation of the cysteine groups. The purities and exact concentrations of the ligand solutions were determined by the Gran method.[26] NaOH was added from a 500 μL micrometer syringe, which was calibrated by both weight titration and the titration of standard materials. The ligand concentrations were 1×10^{-3} M, the Zn^{2+} to ligand, Cd^{2+} to ligand, and Ni^{2+} to ligand molar ratios were 1:1 and 1:2, and the Bi^{3+} to peptide ratios were 1:2 and 1:3. The constants for the hydrolytic Bi^{3+} species were used in these calculations (−1.58 and 0.33 for the formation of $BiOH^{2+}$ and $Bi_6(OH)_{12}^{6+}$ species, respectively).[27] The HYPERQUAD 2006 and SUPERQUAD programs were used for the stability constant calculations.[28,29] Standard deviations were computed by HYPERQUAD 2006 and refer to random errors only.

Mass Spectrometric Measurements. High-resolution mass spectra were obtained on a BrukerQ-FTMS spectrometer (Bruker Daltonik, Bremen, Germany), equipped with an Apollo II electrospray ionization source with an ion funnel. The mass spectrometer was operated in the positive ion mode. The instrumental parameters

were as follows: scan range m/z 400−1600, dry gas nitrogen, temperature 170 °C, ion energy 5 eV. Capillary voltage was optimized to the highest S/N ratio, and it was 4500 V. The small changes of voltage (±500 V) did not significantly affect the optimized spectra. The sample (Bi^{3+}:ligand in a 1:2 stoichiometry, other metals to ligand in a 1:1.1 stoichiometry, [ligand] = 10^{-4} M) was prepared in 1:1 MeOH−H_2O mixture. Variation of the solvent composition down to 5% of MeOH did not change the species composition. The sample was infused at a flow rate of 3 μL/min. The instrument was calibrated externally with the Tunemix mixture (Bruker Daltonik, Germany) in quadratic regression mode. Data were processed by using the Bruker Compass DataAnalysis 4.0 program. The mass

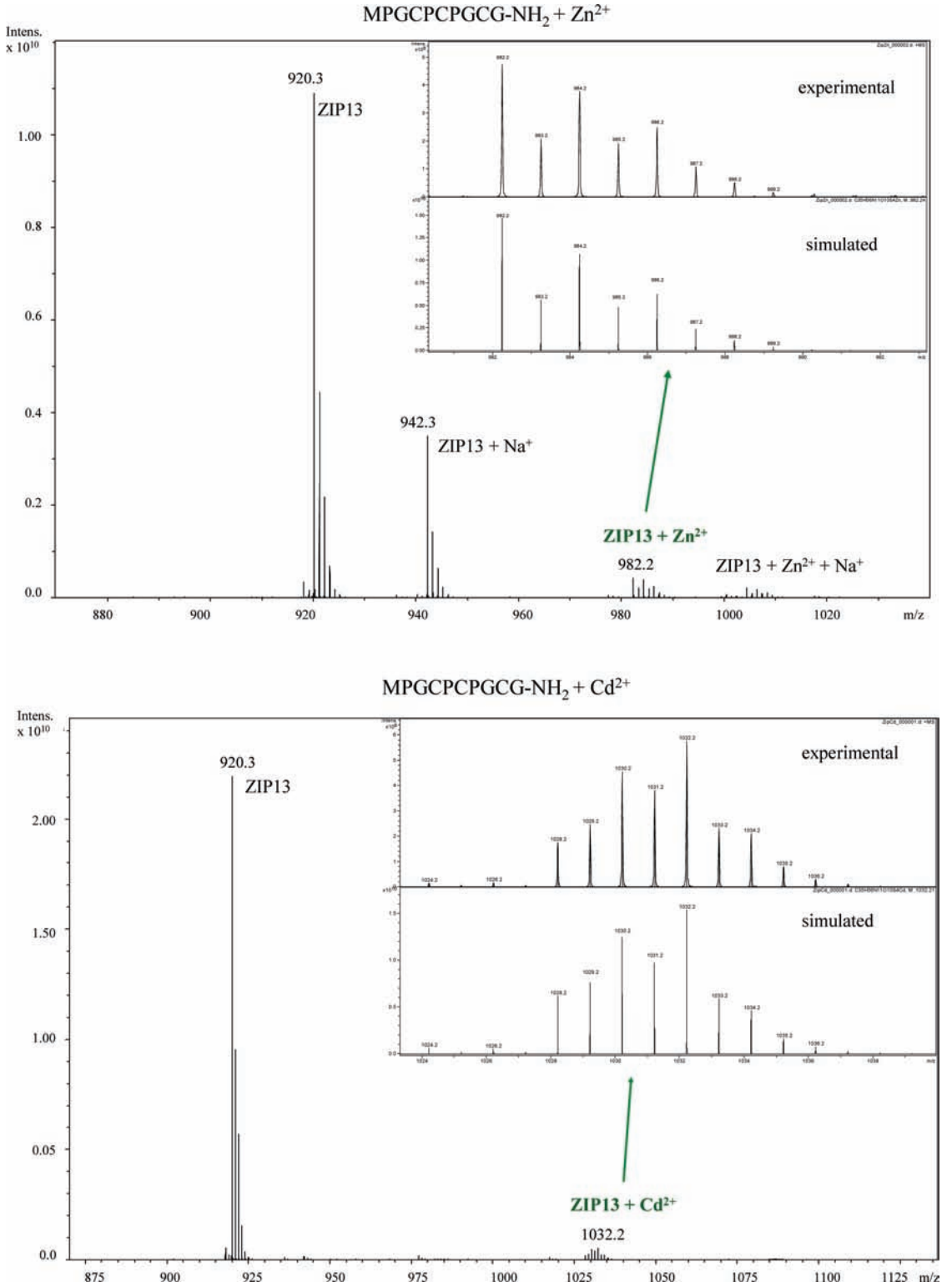

Figure 1. Continued

dx.doi.org/10.1021/ic200270p |*Inorg. Chem.* 2011, 50, 6135–6145

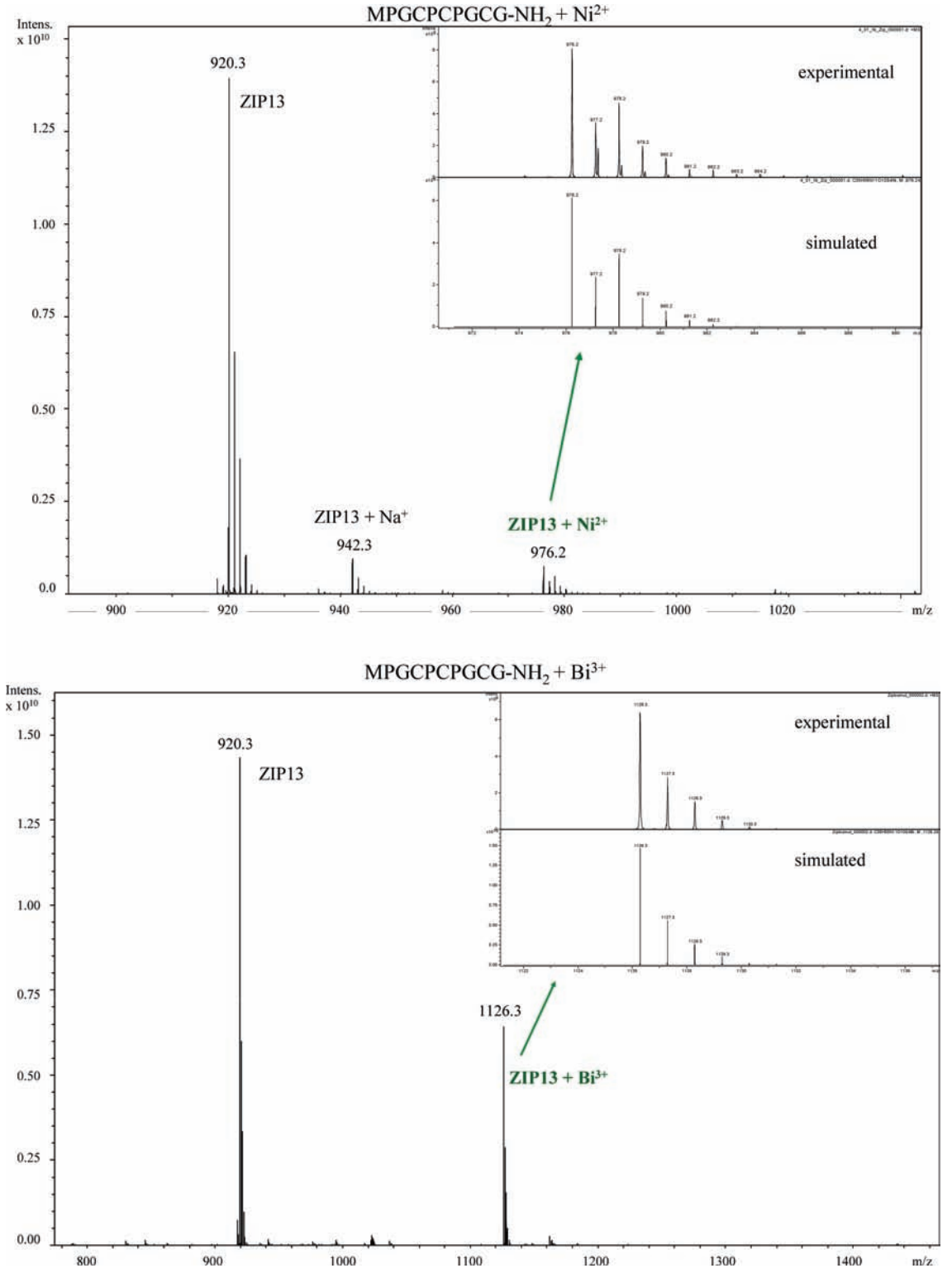

Figure 1. ESI−MS spectra of a system containing MPGCPCPGCG−NH_2 with Zn^{2+}, Cd^{2+}, Ni^{2+}, and Bi^{3+} ions.

accuracy for the calibration was better than 5 ppm, enabling together with the true isotopic pattern (using SigmaFit) an unambiguous confirmation of the elemental composition of the obtained complex.

NMR Measurements. NMR experiments were carried out at 14.1 T at controlled temperature (±0.1 K) on a Bruker Avance 600 MHz equipped with a Silicon Graphics workstation. Suppression of residual water signal was achieved either by presaturation or by excitation sculpting[30] using a selective square pulse on water 2 ms long. Proton resonance assignment was obtained by COSY, TOCSY, NOESY, and ROESY experiments. HSQC experiments were carried out with standard pulse sequences. Spectral processing was performed on a Silicon Graphics O_2 workstation using the XWINNMR 3.6.

RESULTS AND DISCUSSION

Free Ligand. All of the protonation constants of the MPGCPCPGCG−NH_2 peptide arise from the deprotonations of the side chain groups and of the amine group of the peptide. The first three protonation constants (log K = 9.68, 8.77, and 8.17) correspond to the thiolates of the cysteine residues, and the fourth one (6.98) is the result of the association of the proton to the N-terminal amine group of the peptide as it is supported by pH-dependent NMR chemical shift variations detected on Met-1 and Cys protons.

The NMR spectra of the free peptide were performed at pH 5.0, 6.0, 8.5, and 10, which corresponded to the occurrence of predominant metal species. The ^{1}H and ^{13}C chemical shift assignment, obtained at pH 5.0, T 298 K, is reported in Table 1.

Metal Complexes. To determine the stoichiometry, characterize the metal binding sites, and examine the stabilities of the complexes with zinc, nickel, cadmium, and bismuth, mass spectrometry, potentiometry, CD, UV−vis, and NMR spectroscopy have been used.

Mass spectrometry studies have proved the formation of the ZIP13 complex with Zn^{2+}, Cd^{2+}, Ni^{2+}, and Bi^{3+} and showed equimolar binding stoichiometry (Figure 1). Potentiometry, NMR, CD, and UV−vis spectroscopy (the two latter for Ni^{2+} and Cd^{2+} ions) showed very similar binding modes for all four metals. The three thiol side chains of cysteines are involved in metal binding,; the only difference is the stability of the formed complexes (Table 2 and Figure 2).

In the case of the Zn^{2+} complex, the first species, visible at pH 5.5, is ZnHL. In this form, the Zn^{2+} ion is coordinated to three sulfurs from the side chains of cysteine residues as shown by the large NMR line broadening experienced by α and β nuclei of all three Cys. The addition of 1.0 Zn^{2+} equiv caused the complete disappearance of all Cys-4, Cys-6, and Cys-9 correlations in both ^{1}H−^{1}H TOCSY (data not shown) and ^{1}H−^{13}C HSQC (Figure 3A). Beyond the selective effects recorded on Cys

Table 2. Potentiometric Data for Proton, Zn^{2+}, Cd^{2+}, Ni^{2+}, and Bi^{3+} Complexes of MPGCPCPGCG−NH_2 Peptide

	log β	log K
LH	9.68(1)	9.68
LH_2	18.45(1)	8.77
LH_3	26.62(1)	8.17
LH_4	33.60(1)	6.98
ZnHL	22.57(3)	6.61
ZnL	15.96(4)	
CdHL	25.86(2)	6.52
CdL	19.34(3)	
NiHL	19.93(3)	7.21
NiL	12.73(3)	
BiHL	35.79(8)	6.4
BiL	29.39(3)	

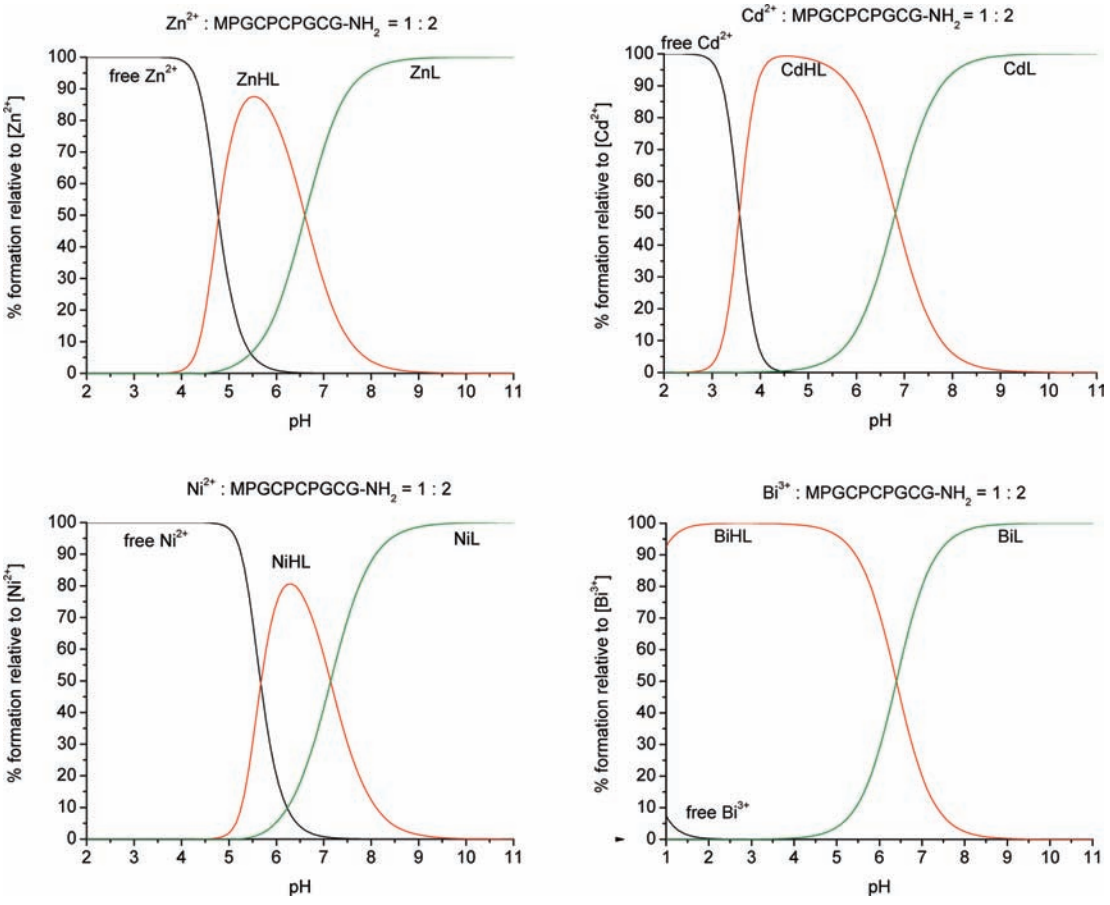

Figure 2. Species distribution profiles for Zn^{2+}, Cd^{2+}, Ni^{2+}, and Bi^{3+} complexes of MPGCPCPGCG−NH_2 peptide. Metal to ligand ratio = 1:2; [metal] = 1×10^{-3} M.

dx.doi.org/10.1021/ic200270p |*Inorg. Chem.* 2011, 50, 6135–6145

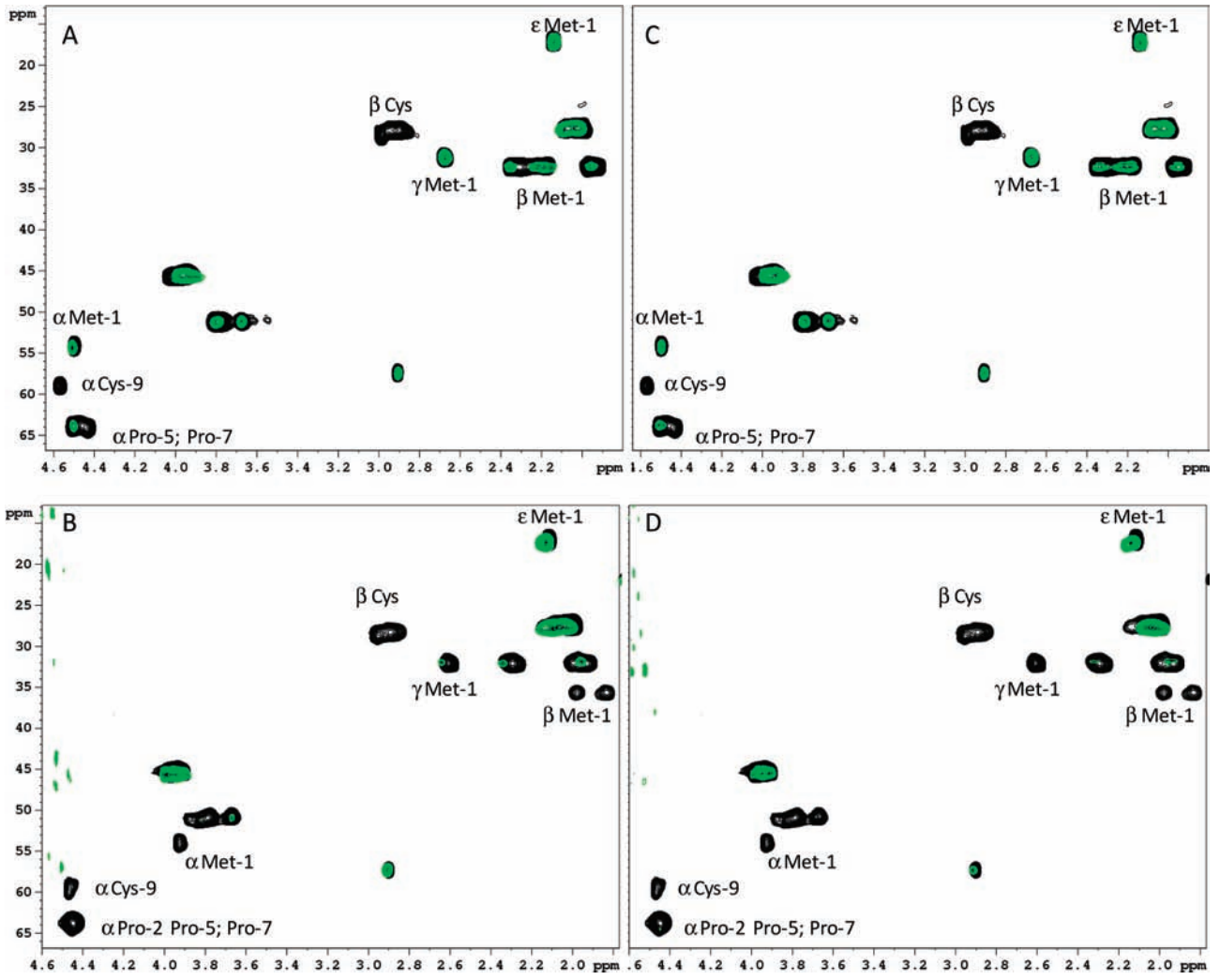

Figure 3. $^{1}H-^{13}C$ HSQC of MPGCPCPGCG−NH_2, 3×10^{-3} M, T = 298 K in the absence (black contours) and in the presence of 1.0 metal equiv (green contours). (A) Zn^{2+}, pH 5.0, (B) Zn^{2+}, pH 8.5, (C) Cd^{2+}, pH 5.0, (D) Cd^{2+}, pH 8.5. The correlation at 2.9, 57 ppm belongs to impurity compounds present in the reference solution used for NMR experiments.

resonances, Pro-5 and Pro-7 cross-peaks were also washed out in the presence of the metal ion. Such behavior, strongly consistent with Zn^{2+} binding to Cys thiol moieties, may be explained by considering the Pro-5 and Pro-7 proximity to metal binding site (Cys-4−Cys-6). The next observed species, ZnL (maximum already at pH 8), have a $\{3S^{-},N_{NH2}\}$ binding mode, with the N-terminal amine being the fourth donor atom, as verified by the additional broadening of α and β Met-1 correlations detected on $^{1}H-^{13}C$ HSQC spectra at pH 8.5 (Figure 3B). The involvement of N-terminus Met-1 is additionally supported by the log K value corresponding to the loss of the N-terminal proton, which is lower than the log K value of the free ligand (6.61 for the deprotonation of the amine in the zinc-bound form, 6.98 for the free peptide).

The Cd^{2+} complex shows a binding mode similar to that of Zn^{2+}. The first three-sulfur complex, CdHL, appears at a lower pH (pH 3) than does the Zn^{2+} complex, indicating, as predicted, a larger stability than that of Zn^{2+}. NMR spectra were very similar to those obtained in the presence of Zn^{2+} (Figure 3C and D), proving a similar binding mode for both metals. Hence, the CdHL and CdL species dominating at pH 5.0 and 8.5, respectively, correspond to Cd^{2+} bound to the three Cys sulfur atoms (pH 5) and with the additional involvement of Met-1 amine group at pH 8.5. As in the previous case, both NMR (Figure 3D) and potentiometry prove the involvement of the α-amine group (log K equals 6.52 for the deprotonation of the N terminus in the cadmium-bound form, while for the free peptide it is 6.98).

As for the Ni^{2+} complex, the first form, NiHL, showed a maximum at pH above 6. Upon Ni^{2+} addition, Cys cross-peaks detected on $^{1}H-^{13}C$ HSQC NMR spectra (Figure 4A) completely disappeared, strongly supporting the metal binding to three sulfurs of the cysteines. Comparable effects were also detected at higher pH (Figure 4B), indicating the unique participation of the three Cys to the Ni^{2+} coordination sphere. To exclude the presence of metal-bound paramagnetic species, reliable with the large ^{1}H and ^{13}C line broadening effects observed, the longitudinal relaxation rates were measured in the presence and in the absence of Ni^{2+} at both pH. The rates obtained for the apo and bound form were almost similar (data not shown), such to exclude the formation of paramagnetic Ni^{2+} complexes.

dx.doi.org/10.1021/ic200270p |*Inorg. Chem.* 2011, 50, 6135–6145

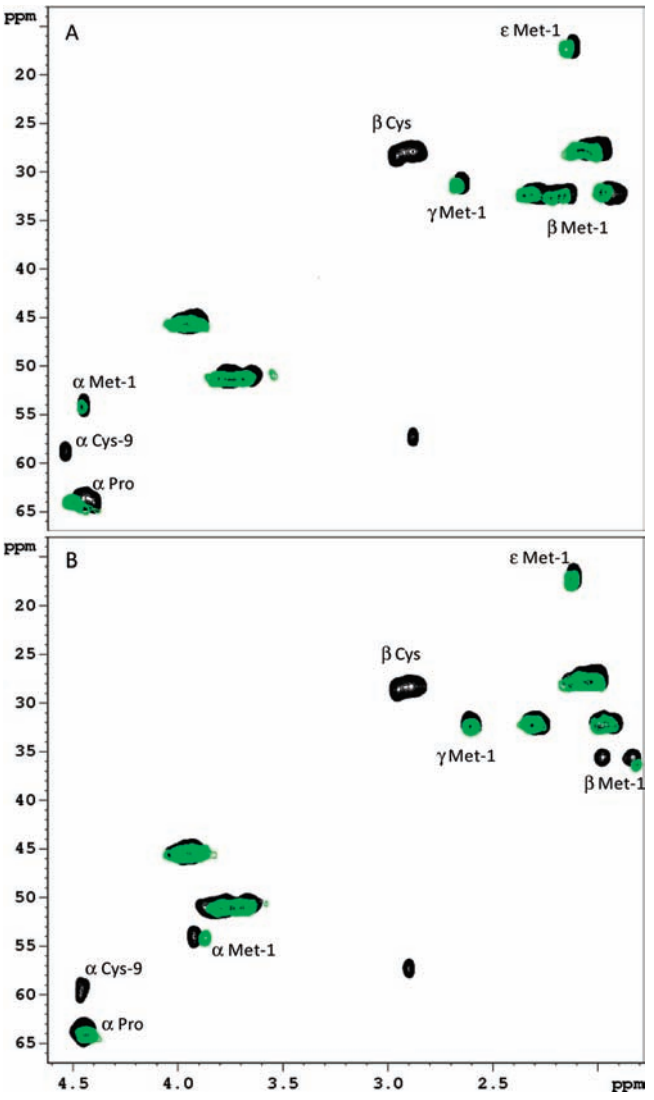

Figure 4. $^{1}H-^{13}C$ HSQC of MPGCPCPGCG−NH_2, 3×10^{-3} M, $T = 298$ K, in the presence (green contours) and in the absence (black contours) of 0.5 Ni^{2+} equiv at pH 6.0 (A) and pH 8.5 (B). The correlation at 2.9, 57 ppm belongs to impurity compounds present in the reference solution used just for free ligand NMR experiments; therefore, its absence in the Ni^{2+} spectra is not due to any metal-induced effect.

The geometries of Zn^{2+} and Cd^{2+} complexes are usually four-coordinate and tend to have a tetrahedral geometry, and we can assume this in our case. UV−vis and CD spectroscopy further prove the proposed binding modes of Ni^{2+} and Cd^{2+}. On the Cd^{2+}−MPGCPCPGCG−NH_2 complex UV−vis plot (Figure 5A), bands below 300 nm, with the maximum at 235 nm, represent charge transfer electronic transition S→Cd^{2+},[31] confirming the effect of Cd^{2+} on cysteine donors. Both CD and UV−vis bands are observed starting from pH 3, which is in good agreement with potentiometric measurements where the first CdHL complex is formed at the same pH (Figure 2). Bands observed between 240 and 260 nm on CD and UV−vis spectra (Figure 5A and B) indicate S→Cd^{2+} charge transfer transition, and their intensities increase with the pH as the formation of Cd^{2+}−MPGCPC-PGCG−NH_2 complexes occurs. In the case of Ni^{2+}−MPGCPC-PGCG−NH_2 complex, UV−vis measurements confirmed the lack of bands with the maximum at 450 nm (Figure 6A), which when present might suggest oxidation of cysteine residues[32] or amide binding. The large enhancement of the S→Ni^{2+} charge transfer transitions in the region of 320−380 nm[33,34] of CD spectra (Figure 6B) further supports the Ni^{2+} complexation to three cysteines. Moreover, the presence of negative circular dichroism extrema from 450 to 490 nm typical of planar, diamagnetic Ni^{2+} peptide complexes[35] strongly indicates a square planar metal geometry (Figure 6B).

The really interesting part of this study appears when we compare the thermodynamic stability of the studied ligand with Zn^{2+} and with Ni^{2+} ions. Ni^{2+} has reasonably high affinity toward thiol sulfurs,[18] and it usually tends to form square planar complexes, in which at least one or two amide nitrogen atoms are involved.[34] Although various studies prove that the stabilities of Zn^{2+} and Ni^{2+} complexes are comparable, especially with sulfur donors,[36] the comparison of such species still remains an important issue for bioinorganic chemists. What is interesting is that the three sulfur-coordinated Zn^{2+} complex is, in all pH range, distinctly more stable than the Ni^{2+} complex (Figure 7), in which the Ni^{2+} ion is bound to the same three sulfur residues. The difference in the ZnL and NiL stability is over 3 orders of magnitude with log β = 15.96 for ZnL and 12.73 for NiL.

What is also worth mentioning, in the case of both Ni^{2+} and Zn^{2+}, is that the coordination of three sulfur atoms from cysteine residues strongly enhances the stability of the formed complexes as it is shown in Figure 8, where the competition plots of Zn^{2+} and Ni^{2+} binding to our ZIP13 fragment and to the N-terminal

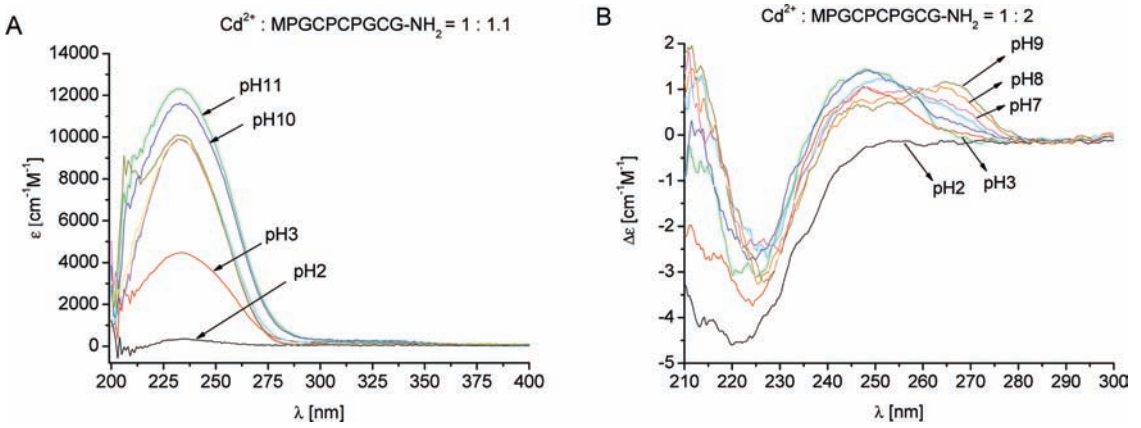

Figure 5. UV−vis (A) and CD spectra (B) for Cd^{2+} complex of MPGCPCPGCG−NH_2 peptide.

dx.doi.org/10.1021/ic200270p |*Inorg. Chem.* 2011, 50, 6135–6145

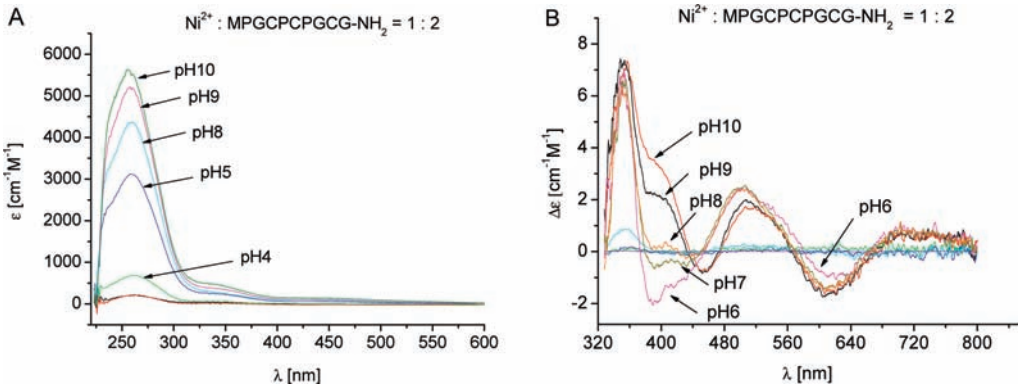

Figure 6. UV−vis (A) and CD spectra (B) for Ni^{2+} complex of MPGCPCPGCG−NH_2 peptide.

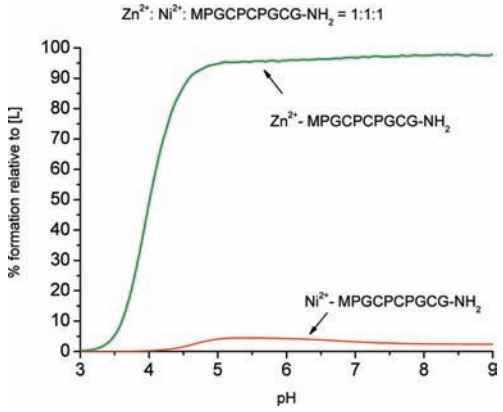

Figure 7. A competition plot of the MPGCPCPGCG−NH_2 peptide with Zn^{2+} and Ni^{2+} (1:1:1 molar ratio).

fragment of human metalothionein-3, MDPETCPCP−NH_2, are reported. Such a comparison gives indirect proof of a 3 Cys $\{3S^-\}$ binding mode in the case of ZIP13 complexes, because their stabilities are much higher when compared to the stabilities of 2-Cys bound ($\{2S^-\}$) complexes.

Bi^{3+} complexes with the studied peptide are the most stable species, when compared to the complexes of Zn^{2+}, Cd^{2+}, and Ni^{2+}. Up to date, both the kinetics and the thermodynamics of solution equilibria for Bi^{3+} are poorly understood. It is clear that hydrolysis can readily dominate the aqueous equilibria of Bi^{3+}, unless it is complexed by an effective ligand. Recent data showed that Bi^{3+} is coordinated by thiol sulfurs of cysteines at an extremely low pH[18,37] and such binding is very efficient to protect against hydroysis.

To calculate the stability constants of Bi^{3+} complexes with the investigated ZIP fragment, potentiometry had to be combined with UV−vis batch titrations, because coordination begins at very low pH. The combined results of the UV−vis and the potentiometric analysis are in perfect agreement with the data obtained from MS and NMR studies and confirm the formation of equimolar complexes.

The distribution diagrams (Figure 2) show that, as in our previous studies,[18] the coordination starts already at pH < 1, preventing the precipitation of Bi^{3+} hydroxyl species. As for the previous metals, the first anchoring sites for Bi^{3+} are three cysteine sulfurs; the UV−vis intensive band (ε = 4500 M^{-1} cm^{-1}) around 350 nm is consistent with the binding of Bi^{3+} to the thiol sulfurs of cysteines. Such thiol-bound species prevail in the solution up to pH 6, that is when dissociation of the amine proton takes place, yet the N-terminal nitrogen does not take part in the binding. The comparison of $^1H-^{13}C$ HSQC and $^1H-^1H$ TOCSY experiments of the apo and Bi^{3+} bound peptide strongly supported the exclusive involvement of all three Cys residues in metal binding at both pH 5.0 and 8.5 (Figures 9 and 10). In fact, Bi^{3+} addition yields selective and exclusive line broadening of all three Cys correlations (Figure 9); moreover, the absence of any key differences between the two investigated pH leads us to exclude the involvement of Met-1 in Bi^{3+} binding at pH 8.5 (Figure 10).

Both the geometry and the coordination number of Bi^{3+} complexes are not exactly clear and can be between 3 and 10. In this case, the coordination number equals three and is in good agreement with the electronic configuration of this metal. We observe no additional deprotonations from bound water molecules. BiL is the most stable complex; it is over 13 orders of magnitude stronger than the most stable CdL species (log β = 35.79 for Bi^{3+} and 22.57 for Cd^{2+} complexes).

Bi^{3+} species can only be compared to other Bi^{3+} species; Figure 11 shows that the $\{3S^-\}$ coordination mode of Bi^{3+}−MPGCPC-PGCG−NH_2 is much stronger than the $\{2S^-,N_{im}\}$ one for the Bi^{3+}−Ac−ACCHDHKKH−NH_2 (C-terminus of *Helicobacter pylori* HspA protein) complex.

Experimental data from all of the used techniques confirmed which side chain groups are the metal binding sites. This knowledge allowed us to propose possible coordination modes for all of the studied complexes. Proposed structures are presented in Figure 12.

CONCLUSIONS

In this work, the structural and thermodynamic properties of Zn^{2+}, Cd^{2+}, Ni^{2+}, and Bi^{3+} complexes with ZIP13 cysteine-rich N-terminal domain have been investigated and compared to each other by using potentiometric and spectroscopic techniques. Full characterization of the complex formation was possible by the correlation of the experimental data obtained from various methods. MS measurements provided the information on the stoichiometry of the interactions, combined UV−vis and potentiometric titrations allowed us to determine the stability constants and pH-dependent species distribution diagrams for the investigated systems, whereas analysis of NMR and CD allowed us to conclude the exact binding sites and the geometry of complex species formed in solution.

dx.doi.org/10.1021/ic200270p |*Inorg. Chem.* 2011, 50, 6135–6145

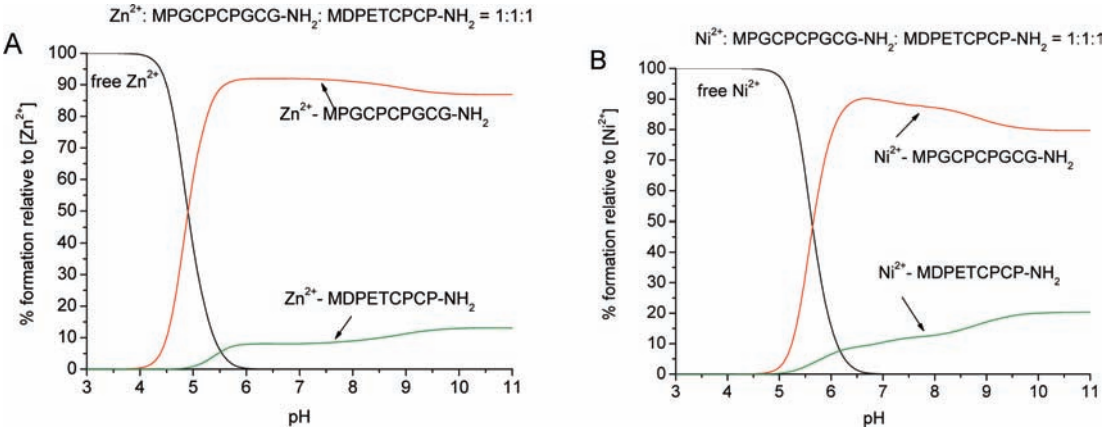

Figure 8. A competition plot of the MPGCPCPGCG−NH_2 and MDPETCPCP−NH_2 peptides with Zn^{2+} (A) and with Ni^{2+} (B) (MPGCPCPGCG−NH_2:MDPETCPCP−NH_2:metal ratio = 1:1:1).

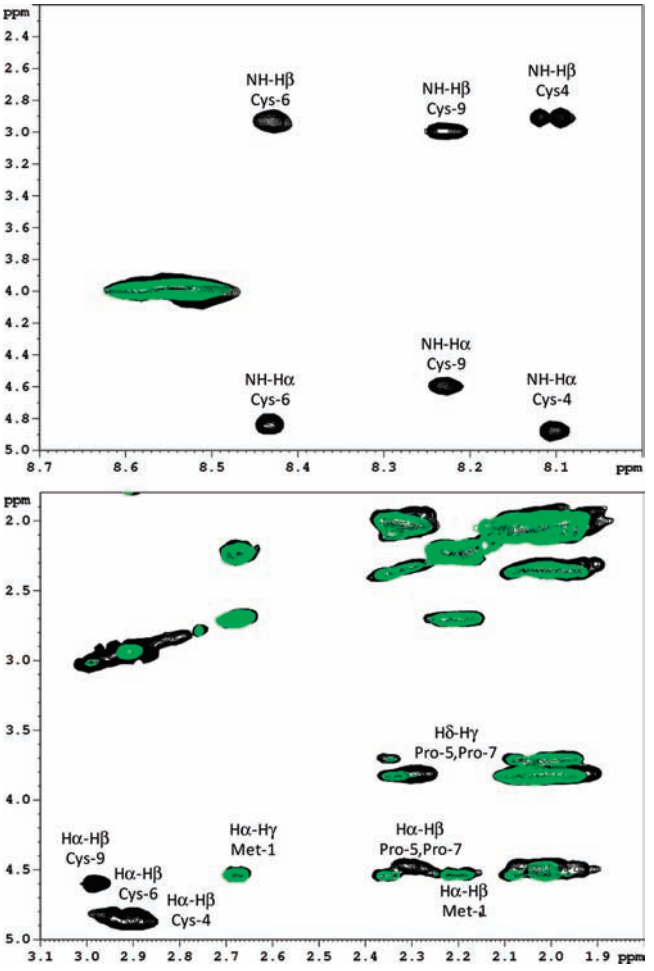

Figure 9. Finger-print and aliphatic regions of $^1H-^1H$ TOCSY spectra of MPGCPCPGCG−NH_2, 3×10^{-3} M, pH 5.0, T = 298 K in the absence (black contours) and in the presence (green contours) of 0.5 Bi^{3+} equiv.

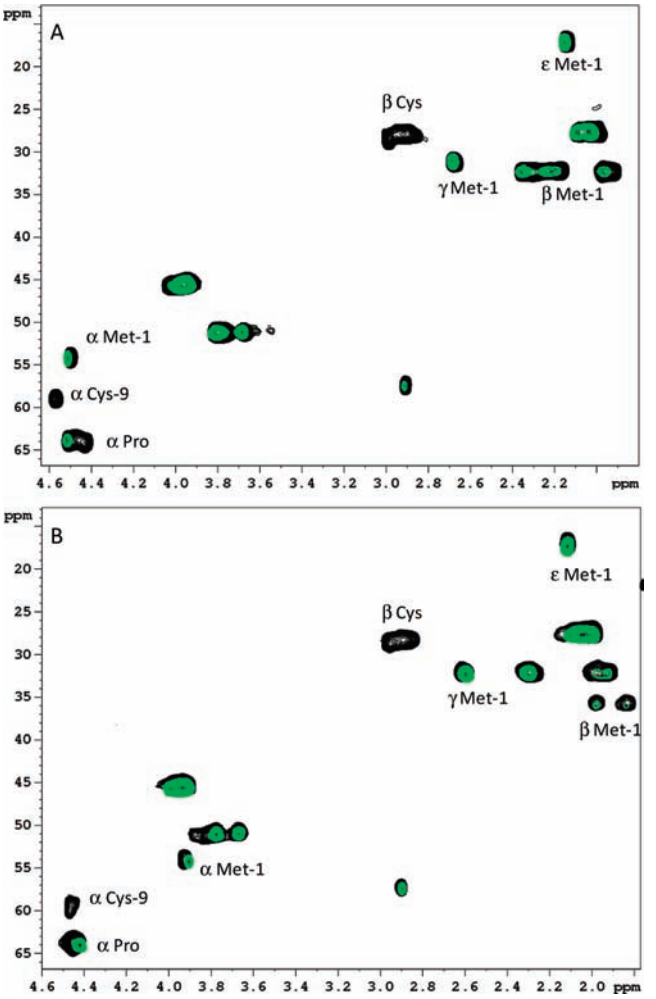

Figure 10. $^1H-^{13}C$ HSQC of MPGCPCPGCG−NH_2, 3×10^{-3} M, T = 298 K in the absence (black contours) and in the presence of 0.5 Bi^{3+} equiv (green contours): pH 5.0 (A), pH 8.5 (B).

At lower pH range, formation of MHL complex species with identical triple thiolate {$3S^-$} donor set has been observed for all of the studied metal ions. Subsequent proton dissociation yields ML species that are present in the pseudophysiological pH range. In the BiL complex, the binding mode does not change with increasing pH; in the case of ZnL and CdL, the fourth coordination residue is the amine group from the unprotected N-terminus of the peptide. Ni^{2+} binding yields the diamagnetic complex

dx.doi.org/10.1021/ic200270p |*Inorg. Chem.* 2011, 50, 6135–6145

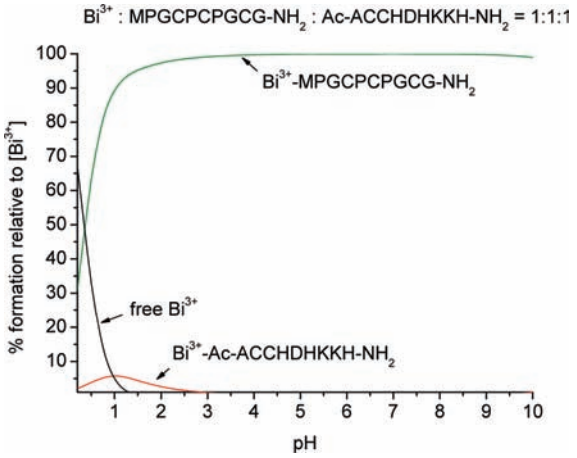

Figure 11. A competition plot of the MPGCPCPGCG−NH_2 and Ac−ACCHDHKKH−NH_2 peptides with Bi^{3+} (1:1:1 molar ratio).

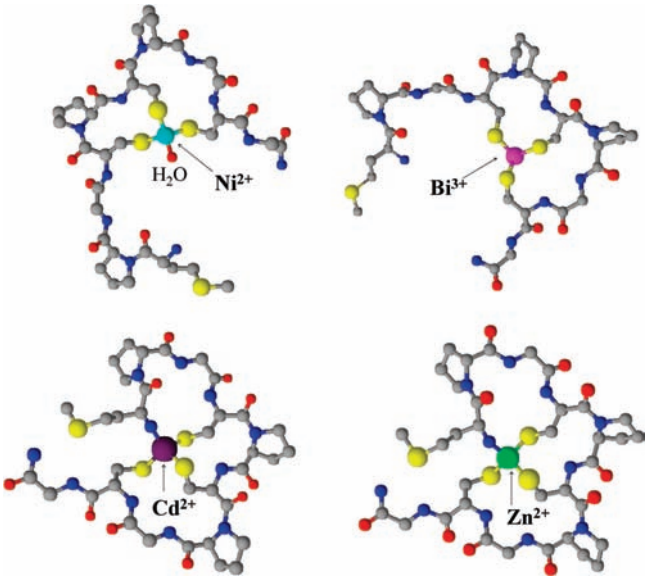

Figure 12. Proposed structures of BiL, CdL, NiL, and ZnL complexes; L is the N-terminus of ZIP13 (MPGCPCPGCG−NH_2). For clearer imaging, the hydrogens were removed; colors: silver, carbon; blue, nitrogen; red, oxygen; yellow, sulfur. Figures were prepared in ACDLABS 12.0 (ChemSketch 3D).

species with three thiolates involved in the coordination of single metal ion. Because no further peptidic binding group has been identified, we suppose that the equatorial coordination sphere is completed by water molecule. Three thiolate sulfur atoms provide enough stability to maintain pseudoplanar geometry of the metal ion.

Although the three cysteines were found to constitute the metal binding domain for all of the investigated metals, the comparison of the metal complex stabilities indicated that the Bi^{3+} is absolutely the most efficient metal ion and that, on the other hand, Ni^{2+} complexes are the weakest ones.

Finally, the comparison between the thermodynamic and structural properties of Zn^{2+}, Ni^{2+}, and Bi^{3+} complexes interacting with ZIP13 or other different peptide fragments indicated that the involvement of three Cys sulfur atoms results in much more stable complexes as compared to those where only two Cys thiols are bound.

The stability of the metal ions complexes of ZIP13 N-terminus decreases in the series $Bi^{3+} \gg Cd^{2+} > Zn^{2+} > Ni^{2+}$. Bismuth has the strongest affinity for the studied sequence of ZIP13. What might have been surprising is that stronger complexes are formed by Zn^{2+} than by Ni^{2+}. The coordination of the N-terminal amino group stabilizes additionally Zn^{2+} complexes when compared to Ni^{2+} (Figure 7). As expected, Cd^{2+} complexes are thermodynamically more stable than Zn^{2+} species. Also, an extra cysteinyl residue has a stabilizing effect on the complexes. Such 3Cys- to 2Cys-containing systems comparative studies (Figures 8 and 11) further confirm the involvement of all three thiol groups in metal binding. The obtained results not only provide some insight into the biological chemistry of Cys-rich peptide fragments, but also give information about the coordination modes associated with them.

AUTHOR INFORMATION

Corresponding Author

*E-mail: henrykoz@wchuwr.pl.

ACKNOWLEDGMENT

This work was supported by the Polish State Committee for Scientific Research (KBN N N204 146537 and KBN N N204 183340).

REFERENCES

(1) Schmitt-Ulms, G.; Ehsani, S.; Watts, J. C.; Westaway, D.; Wille, H. *PLoS One* **2009**, *4*, e7208.
(2) Giese, A.; Levin, J.; Bertsch, U.; Kretzschmar, H. *Biochem. Biophys. Res. Commun.* **2004**, *320*, 1240–1246.
(3) Jobling, M. F.; Huang, X.; Stewart, L. R.; Barnham, K. J.; Curtain, C.; Volitakis, I.; Perugini, M.; White, A. R.; Cherny, R. A.; Masters, C. L.; Barrow, C. J.; Collins, S. J.; Bush, A. I.; Cappai, R. *Biochemistry* **2001**, *40*, 8073–8084.
(4) Grass, G.; Wong, M. D.; Rosen, B. P.; Smith, R. L.; Rensing, C. *J. Bacteriol.* **2002**, *184*, 864–866.
(5) Dufner-Beattie, J.; Wang, F.; Kuo, Y. M.; Gitschier, J.; Eide, D.; Andrews, G. K. *J. Biol. Chem.* **2003**, *278*, 33474–33481.
(6) Palmiter, R. D.; Huang, L. *Eur. J. Physiol.* **2004**, *447*, 744–751.
(7) Eide, D. J. *Eur. J. Physiol.* **2004**, *447*, 796–800.
(8) Liuzzi, J. P.; Cousins, R. J. *Annu. Rev. Nutr.* **2004**, *24*, 151–172.
(9) Sim Franklin, R. B.; Feng, P.; Milon, B.; Desouki, M. M.; Singh, K. K.; Kajdacsy-Balla, A.; Bagasra, O.; Costello, L. C. *Mol. Cancer* **2005**, *4*, 32–45.
(10) Kelleher, S. L.; Lonnerdal, B. *Am. J. Physiol.* **2005**, *288*, C1042–C1047.
(11) Taylor, K. M. *IUBMB Life* **2000**, *49*, 249–253.
(12) Gaither, L. A.; Eide, D. J. *J. Biol. Chem.* **2001**, *276*, 22258–22264.
(13) Gaither, L. A.; Eide, D. J. *J. Biol. Chem.* **2000**, *275*, 5560–5564.
(14) Wang, F.; Kim, B. E.; Petris, M. J.; Eide, D. J. *J. Biol. Chem.* **2004**, *279*, 51433–51441.
(15) Ramesh, S. A.; Shin, R.; Eide, D. J.; Schachtman, D. P. *Plant Physiol.* **2003**, *133*, 126–134.
(16) Kulon, K.; Valensin, D.; Kamysz, W.; Valensin, G.; Nadolski, P.; Porciatti, E.; Gaggelli, E.; Kozłowski, H. *J. Inorg. Biochem.* **2008**, *102*, 960–972.
(17) Valensin, D.; Szyrwiel, L.; Camponeschi, F.; Rowińska-Żyrek, M.; Molteni, E.; Jankowska, E.; Szymanska, A.; Gaggelli, E.; Valensin, G.; Kozłowski, H. *Inorg. Chem.* **2009**, *48*, 7330–7340.

(18) Rowinska-Zyrek, M.; Witkowska, D.; Valensin, D.; Kamysz, W.; Kozłowski, H. *Dalton Trans.* **2010**, *39*, 5814–5826.
(19) Dalton, T. P.; He, L.; Wang, B.; Miller, M. L.; Jin, L.; Stringer, K. F.; Chang, X.; Baxter, C. S.; Nebert, D. W. *Proc. Natl. Acad. Sci. U.S.A.* **2005**, *102*, 3401–3406.
(20) He, L.; Wang, B.; Hay, E. B.; Nebert, D. W. *Toxicol. Appl. Pharmacol.* **2009**, *238*, 250–257.
(21) Kusters, J.; Vliet, A.; Kuipers, E. *Clin. Microbiol. Rev.* **2006**, *19*, 449.
(22) Fukada, T.; Civic, N.; Furuichi, T.; Shimoda, S.; Mishima, K. et al. *PLoS One* **2008**, *3*, e3642.
(23) Binstead, R.; Jung, B.; Zuberbühler, A. *SPECFIT/32 Global Analysis System, Version 3.0*; Spectrum Software Associates: Marlborough, MA, 2000.
(24) Gampp, H.; Maeder, M.; Meyer, Ch. J.; Zuberbühler, A. *Anal. Chim. Acta* **1987**, *193*, 287–293.
(25) Irving, H.; Miles, M.; Pettit, L. *Anal. Chim. Acta* **1967**, *38*, 475–488.
(26) Gran, G. *Acta Chem. Scand.* **1950**, *4*, 559–577.
(27) Pettit, L. D.; Powell, H. *The IUPAC Stability Constants Q1 Database*; London, UK, 1992−2002.
(28) Gans, P.; Sabatini, A.; Vacca, A. *J. Chem. Soc., Dalton Trans.* **1985**, 1195–1200.
(29) Gans, P.; Sabatini, A.; Vacca, A. *Talanta* **1996**, *43*, 1739–1753.
(30) Hwang, T.; Shaka, A. *J. Magn. Reson., Ser. A* **1995**, *112*, 275–279.
(31) Chen, X.; Chu, M.; Giedroc, D. P. *JBIC, J. Biol. Inorg. Chem.* **2000**, *5*, 93–101.
(32) Ross, S. A.; Burrows, C. K. *Inorg. Chem.* **1998**, *37*, 5358–5363.
(33) Formicka-Kozlowska, G.; Kozłowski, H.; Jezowska-Trzebiatowska, B. *Inorg. Chim. Acta* **1977**, *25*, 1–9.
(34) Cherifi, K.; Decock-Le Reverend, B.; Varnagy, K.; Kiss, T.; Sovago, I.; Loucheux, C.; Kozłowski, H. *J. Inorg. Biochem.* **1990**, *38*, 69–80.
(35) Chang, J.; Martin, R. B. *J. Phys. Chem.* **1969**, *73*, 4277–4283.
(36) Sóvágó, I.; Gergely, A.; Harman, B.; Kiss, T. J. *Inorg. Nucl. Chem.* **1979**, *41*, 1629–1633.
(37) Rowinska-Zyrek, M.; Valensin, D.; Szyrwiel, L.; Grzonka, Z.; Kozłowski, H. *Dalton Trans.* **2009**, *42*, 9131–9140.